

# Lectures on Landau Hydrodynamics\*

Cheuk-Yin Wong<sup>†</sup>

*Physics Division, Oak Ridge National Laboratory, Oak Ridge, TN 37831*

(Dated: November 6, 2018)

Landau hydrodynamics is a plausible description for the evolution of the dense hot matter produced in high-energy heavy-ion collisions. We review the formulation of Landau hydrodynamics to pave the way for its application in high-energy heavy-ion collisions. It is found that Landau's rapidity distribution needs to be modified to provide a better quantitative description. In particular, the rapidity distribution in the center-of-mass system should be more appropriately given as  $dN/dy \propto \exp\{\sqrt{y_b^2 - y^2}\}$ , where  $y_b = \ln\{\sqrt{s_{NN}}/m_p\}$  is the beam nucleon rapidity, instead of Landau's original result of  $dN/dy(\text{Landau}) \propto \exp\{\sqrt{L^2 - y^2}\}$  where  $L = \ln\{\sqrt{s_{NN}}/2m_p\}$ . The modified distribution is compared with the Landau distribution and experimental data. It is found that the modified distribution agrees better with experimental  $dN/dy$  data than the Landau distribution and it differs only slightly from the Landau Gaussian distribution  $dN/dy(\text{Landau Gaussian}) \propto \exp\{-y^2/2L\}$ . Past successes of the Gaussian distribution in explaining experimental rapidity data arises, not because it is an approximation of the original Landau distribution, but because it is in fact a close representation of the modified distribution.

PACS numbers: 25.75.-q 25.75.Ag

## I. INTRODUCTION

The evolution of the dense hot matter produced in high-energy heavy-ion collisions is a problem of intrinsic interest. In many problems in high-energy heavy-ion collisions, such as in the investigation of the fate of a heavy quarkonium in quark-gluon plasma and the interaction of a jet with the produced medium, it is desirable to have a good description of the dynamics of the matter produced in the collision. For these problems, Landau hydrodynamics [1, 2] furnishes a plausible description for the evolution of an assembly of dense matter at a high temperature and pressure. Its dynamics during the first stage of one-dimensional longitudinal expansion can be solved exactly [2, 3, 4, 5, 6, 7, 8, 9, 10, 11, 12]. The one-dimensional longitudinal expansion problem admits an approximate solution that is applicable to the bulk part of the fluid. The subsequent three-dimensional motion can be solved approximately to give rise to predictions that come close to experimental data [13, 14, 15, 16]. A thorough understanding and critical tests of the model will make it a useful tool for the description of the evolution of the produced dense matter. We therefore review the formulation of Landau hydrodynamics to pave the way for its quantitative applications in high-energy heavy-ion collisions.

Common to both Landau hydrodynamics and Bjorken hydrodynamics is the basic assumption that in the dense hot matter produced in high-energy heavy-ion collisions, the density of the quanta of the medium (either quarks and gluons or the hadrons) is so high that the mean-free paths of the constituents are short, and a state of local thermal equilibrium can be maintained through out. Such a condition may be at hand in collisions at very high energies. Under the circumstances, the dynamics of the system will be determined by the equation of hydrodynamics possessing local thermal equilibrium. As we are dealing with high temperatures and high densities for which the temperature is of the order of the rest mass of the quanta, we need to examine the problem with relativistic hydrodynamics.

The major difference between Landau hydrodynamics and Bjorken hydrodynamics is in the nature

---

\* Lectures presented at the Helmholtz International Summer School, Bogoliubov Laboratory of Theoretical Physics, JINR, Dubna, July 14-26, 2008

<sup>†</sup> wongc@ornl.gov

of the flow. In Bjorken hydrodynamics, boost invariance is assumed so that the energy density  $\epsilon$  is independent of the rapidity. It is a function of the proper time  $\tau$  only,  $\epsilon_{\text{Bjorken}}(\tau)$ . However, in Landau hydrodynamics, no such an assumption is made, and the energy density is a local function of spatial and temporal coordinates,  $\epsilon_{\text{Landau}}(t, z, x, y)$ .

We can consider collisions of two equal-size nuclei of diameter  $a$ . The disk of initial configuration in the center-of-mass system has a longitudinal thickness  $\Delta$  given by

$$\Delta = a/\gamma, \quad (1.1)$$

where  $\gamma$  is the Lorentz contraction factor

$$\gamma = \frac{\sqrt{s_{NN}}}{2m_p}, \quad (1.2)$$

$\sqrt{s_{NN}}/2$  is the center-of-mass energy per nucleon, and  $m_p$  is the proton mass. The dimensions of the disk are not symmetrical in the longitudinal and transverse directions. The initial configuration can be depicted as in Fig. 1 where it can be represented as an elliptical disk with a thickness  $\Delta$  and major diameters  $a_x$  and  $a_y$ , with the reaction plane lying on the  $x$ - $z$  plane. Depending on the impact parameter, the dimensions of the disk obey  $a_x \leq a_y \leq a$ , and the azimuthal radius  $a_\phi/2$  depends on the azimuthal angle  $\phi$  measured from the  $x$ -axis. For a central collision,  $a_x = a_y = a$ .

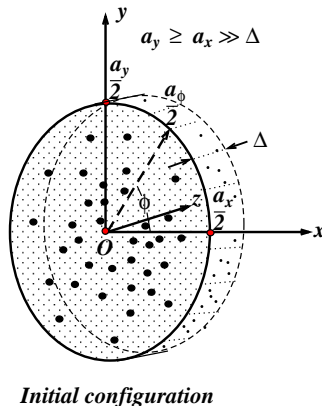


FIG. 1: Initial configuration in the collision of two heavy nuclei in the center-of-mass system. The region of nuclear overlap consists of a thin disk of thickness  $\Delta$  along the longitudinal  $z$ -axis. The reaction plane is designated to lie on the  $x$ - $z$  plane, and the transverse radii are  $a_x/2$  and  $a_y/2$ .

The matter in the disk can be described as a fluid with an energy density field  $\epsilon$ , and a 4-velocity field  $u^\mu$ . In the center-of-mass system to which we focus our attention, the disk of matter can be considered to be initially nearly at rest. The density of the produced matter and its associated pressure are very large, whereas the spatial dimensions of the fluid are very small. As a consequence, large pressure gradients are generated. The generated pressure gradients lead to the subsequent expansion of the system in all directions.

In highly relativistic collisions to which we focus our attention, the center-of-mass energy per nucleon is much greater than the nucleon rest mass,  $(\sqrt{s_{NN}}/2) \gg m_p$ . We have then  $\Delta \ll a_x \leq a_y$  and  $\nabla_z p \gg \nabla_x p \geq \nabla_y p$ . The pressure gradient in the longitudinal  $z$  direction far exceeds those along the transverse  $x$  and  $y$  directions. The expansion along the longitudinal direction proceeds much faster than the transverse expansions. Among the two transverse directions, the expansion along the  $x$  direction proceeds slightly faster than the expansion along the  $y$  direction, leading to the presence of the elliptic flow.

The large difference of the expansion speeds in the longitudinal and transverse directions allows Landau to split the evolution dynamics into two stages. In the first stage, one considers a one-dimensional longitudinal expansion in conjunction with a simultaneous but slower transverse expansion. The second stage occurs when the transverse displacement exceeds the initial transverse dimensions so that the transverse force acting on the fluid element become so small as to be negligible. Thus, in the second stage, the fluid element will freeze its rapidity to stream out in a conic flight with a fixed polar angle. The magnitude of the transverse displacement decreases with increasing rapidity magnitudes. Therefore different parts of the fluid will enter from the first stage to the second stage at different times. Those fluid elements with the smallest rapidity magnitude will enter the second stage the earliest while those elements with the largest rapidity magnitude will enter the second stage the latest. By matching the solutions for the first and the second stages, the dynamics of the system can be followed, up to the end point of the hydrodynamical evolution.

Recent comparison with experimental data indicates that the Landau hydrodynamical model yields results that agree with experiment. In Refs. [13, 14, 15, 17], quantitative analyses use an approximate form of the Landau rapidity distribution [1, 2],

$$dN/dy \propto \exp\{-y^2/2L\}, \quad (1.3)$$

where  $L$  is the logarithm of the Lorentz contraction factor  $\gamma$

$$L = \ln \gamma = \ln(\sqrt{s_{NN}}/2m_p). \quad (1.4)$$

This Gaussian form of the rapidity distribution gives theoretical rapidity widths that agree with experimental widths for many different particles in central AuAu collisions, to within 5 to 10%, from AGS energies to RHIC energies [13, 14, 15]. The Landau hydrodynamical model also gives the correct energy dependence of the observed total multiplicity, and it exhibits the property of “limiting fragmentation” at forward rapidities [14, 15]. A similar analysis in terms of the pseudorapidity variable  $\eta$  at zero pseudorapidity has been carried out in [18].

The successes of these quantitative and qualitative analyses indicate that Landau hydrodynamics can be a reasonable description. However, they also raise many unanswered questions. Firstly, the original Landau result stipulates the rapidity distribution to be [1, 2]

$$dN/d\lambda(\text{Landau}) \propto \exp\{\sqrt{L^2 - \lambda^2}\}, \quad (1.5)$$

where the symbol  $\lambda$  is often taken to be the rapidity variable  $y$  [13, 14, 15, 17]. In the original work of Landau and his collaborator in [1, 2], the variable  $\lambda$  is used to represent the polar angle  $\theta$  as  $e^{-\lambda} = \theta$ ; there is the question whether the variable  $\lambda$  in the Landau rapidity distribution (1.5) should be taken as the rapidity variable  $y$  [13, 14, 15, 17] or the pseudorapidity variable  $\eta$  [18] appropriate to describe the polar angle. Such a distinction between the rapidity and pseudorapidity variables is quantitatively important because the shape of the distributions in these two variables are different near the region of small rapidities [19]. Secondly, the Gaussian rapidity distribution (1.3) used in the analyses of Refs. [13, 14, 15], as well as in the earlier work of [17], is only an approximation of the original Landau distribution of Eq. (1.5). The Gaussian approximation is valid only for  $\lambda \ll L$ , when we expand the square-root function in powers of  $\lambda/L$ . There is the question whether it is appropriate to apply the Gaussian distribution (1.3) to the whole range of  $\lambda$ , including the region of  $\lambda$  for which the expansion condition  $\lambda \ll L$  is not satisfied. The Landau distribution (1.5) and the Gaussian distribution (1.3) are in fact different distributions. While the original Landau distribution may be considered to receive theoretical support in Landau hydrodynamics as justified in Refs. [1, 2], a firm theoretical foundation for the Gaussian distribution (1.3) in Landau hydrodynamics is still lacking. Finally, if one does not make the expansion of the square-root function and one keeps the original

Landau distribution of Eq. (1.5), then there is the quantitative question [20] whether this original Landau distribution with the theoretical  $L$  value will give results that agree with experimental data.

In view of the above unanswered questions, our task in reviewing the Landau hydrodynamical model will need to ensure that we are dealing with the rapidity variable  $y$  and not the pseudorapidity variable. We need to be careful about various numerical factors so as to obtain a quantitative determination of the parameters in the final theoretical results. Finally, we need to ascertain whether the theoretical results agree with experimental data. If we succeed in resolving these questions, we will pave the way for its future application to other problems in high-energy heavy-ion collisions.

## II. TOTAL NUMBER OF PRODUCED PARTICLES

Before we study the dynamics in detail, we would like to examine the total number of particles produced in a central heavy-ion collision in Landau hydrodynamics. Landau assumed that the hydrodynamical motion of the fluid after the initial collision process is adiabatic. He argued that the only thing that can destroy adiabaticity would be the shock wave. They occur at the initial compressional stage of the collision process [21]. It is hard to imagine how they could be formed in the bulk part during the subsequent expansion phase after the initial compression and thermalization. Landau therefore assumed that during the longitudinal and transverse expansion phase under consideration, the entropy content of the the individual region remains unchanged. The total entropy of the system is therefore unchanged and can be evaluated at the initial stage of the overlapped and compressed system.

The total entropy content is a very useful quantity because it is closely related to the total particle number. From the consideration of the thermodynamical properties of many elementary systems, Landau found that the ratio of the entropy density to the number density for a thermally equilibrated system is nearly a constant within the temperature region of interest. Landau therefore postulated that the number density is proportional to the entropy density. Thus, by collecting all fluid elements, the total number of particles is proportional to the total entropy. As the total entropy of the system is unchanged during the hydrodynamical evolution, the total number of observed particles can be determined from the initial entropy of the system.

We work in the center-of-mass system and consider the central collision of two equal nuclei, each of mass number  $A$ , at a nucleon-nucleon center-of-mass energy  $\sqrt{s_{NN}}$ . Consider first the case of central AA collisions with  $A \gg 1$  such that nucleons of one nucleus collide with a large numbers of nucleons of the other nucleus and the whole energy content is used in particle production. This is the case of “full stopping”. The total energy content of the system is

$$E = \sqrt{s_{NN}}A. \quad (2.1)$$

The initial compressed system is contained in a volume that is Lorentz contracted to

$$V = \frac{4\pi}{3}(a/2)^3/\gamma, \quad (2.2)$$

where the nuclear radius  $a/2$  is related to the mass number by

$$a/2 = r_0 A^{1/3}, \quad (2.3)$$

and  $r_0 = 1.2$  fm. The energy density of the system is therefore

$$\epsilon = E/V = \gamma\sqrt{s_{NN}}/(4\pi r_0^3/3), \quad (2.4)$$

which is independent of  $A$  and depends on energy as  $s_{NN}$ . For a system in local thermal equilibrium, the entropy density  $\sigma$  is related to the energy density by

$$\sigma = \text{constant } \epsilon^{3/4}. \quad (2.5)$$

The total entropy content of the system is therefore

$$S = \sigma V = \text{constant } s_{NN}^{1/4} A. \quad (2.6)$$

With Landau's assumption relating entropy and particle number,  $N \propto S$ , the total number of particles produced is

$$N \propto s_{NN}^{1/4} A, \quad (2.7)$$

and the total number of produced charged particles per participant pair is

$$N_{\text{ch}}/A = N_{\text{ch}}/(N_{\text{part}}/2) = K(\sqrt{s_{NN}}/\text{GeV})^{1/2}, \quad (2.8)$$

where  $K$  can be determined phenomenologically by comparison with experimental data.

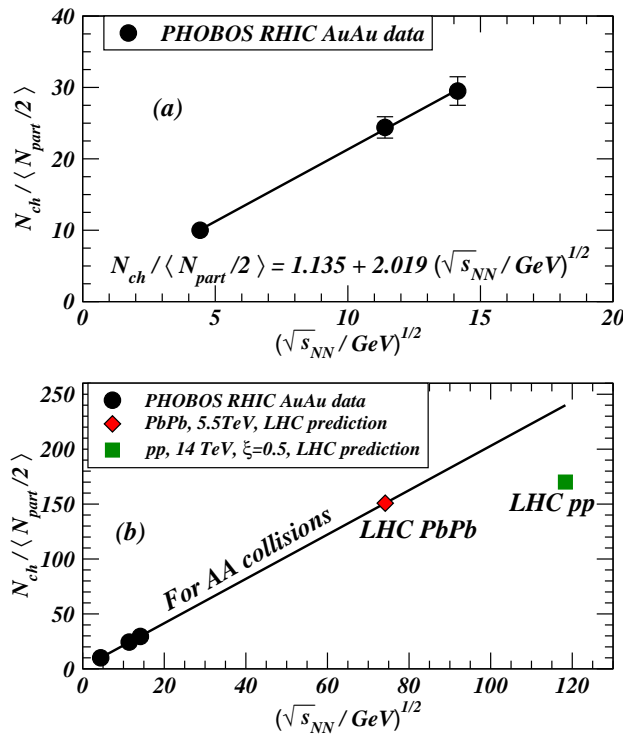


FIG. 2: Total number of produced charged particles per pair of participants,  $N_{\text{ch}}/(N_{\text{part}}/2)$ , as a function of  $(\sqrt{s_{NN}}/\text{GeV})^{1/2}$ . (a) PHOBOS data  $N_{\text{ch}}/(N_{\text{part}}/2)$  data for central AuAu collisions at different  $(\sqrt{s_{NN}}/\text{GeV})^{1/2}$  and the Landau hydrodynamical model fit, and (b) the extrapolation of the Landau hydrodynamical model to LHC energies.

In Fig. 1(a), we show the PHOBOS data of  $N_{\text{ch}}/(N_{\text{part}}/2)$  as a function of  $(\sqrt{s_{NN}}/\text{GeV})^{1/2}$  for central AuAu collisions in RHIC [14, 15, 16]. The RHIC AuAu data can be parametrized as

$$N_{\text{ch}}/(N_{\text{part}}/2) = 1.135 + 2.019(\sqrt{s_{NN}}/\text{GeV})^{1/2}, \quad (2.9)$$

where the constant 1.135 arise from the leading nucleons. The constant  $K$  as determined from the data is  $K = 2.018$  which agrees with the earlier estimate of  $K = 2$  [1, 2].

Consider next pp and p $\bar{p}$  collisions in which not all the energy of  $\sqrt{s_{NN}}$  is used in particle production, as the leading particles carry a substantial fraction of the initial energy. If we denote the particle production energy fraction in pp and p $\bar{p}$  collisions by  $\xi$ , then Eq. (2.8) is modified to be

$$N_{\text{ch}} = K(\xi\sqrt{s_{NN}}/\text{GeV})^{1/2}. \quad (2.10)$$

Comparison of the charged particle multiplicity in pp, p $\bar{p}$ , and  $e^+e^-$  collisions indicates that the particle production energy fraction  $\xi$  for pp and p $\bar{p}$  collisions is approximately 0.5 [14, 15, 19, 22]. In contrast, the case of RHIC AA data in high-energy heavy-ion collisions corresponds to full nuclear stopping with  $\xi = 1$  [14, 15].

In Fig. 1(b), we show the predictions for the charge particle multiplicity per pair of participants for collisions at LHC energies. For pp collisions at 14 TeV with a particle production energy fraction  $\xi = 0.5$ ,  $N_{\text{ch}}$  is predicted to be 170. For central PbPb collisions at  $\sqrt{s_{NN}} = 5.5$  TeV with full nuclear stopping ( $\xi = 1$ ),  $N_{\text{ch}}/(N_{\text{part}}/2)$  is predicted to be 151.

### III. LONGITUDINAL HYDRODYNAMICAL EXPANSION

We proceed to examine the dynamics of the longitudinal and transverse expansions. Among the coordinates  $(t, z, x, y) \equiv (x^0, x^1, x^2, x^3)$  used as the arena to describe the fluid, Landau suggested a method to split the problem into two stages. The first stage consists of simultaneous and independent expansions along the longitudinal and the transverse directions. For the one-dimensional longitudinal expansion, the equation of hydrodynamics is

$$\frac{\partial T^{00}}{\partial t} + \frac{\partial T^{01}}{\partial z} = 0, \quad (3.1)$$

$$\frac{\partial T^{01}}{\partial t} + \frac{\partial T^{11}}{\partial z} = 0, \quad (3.2)$$

where

$$T^{\mu\nu} = (\epsilon + p)u^\mu u^\nu - pg^{\mu\nu}. \quad (3.3)$$

In hydrodynamical calculations, we need an equation of state. We shall assume for simplicity the relativistic equation of state

$$p = \epsilon/3, \quad (3.4)$$

which allows one to express the local pressure  $p$  as a function of the energy density  $\epsilon$ . It is convenient to represent the velocity fields  $(u^0, u^1)$  by the flow rapidity  $y$

$$u^0 = \cosh y, \quad (3.5a)$$

$$u^1 = \sinh y. \quad (3.5b)$$

In this form, the property of the velocity fields,  $(u^0)^2 - (u^1)^2 = 1$ , is readily satisfied. A particle of mass  $m$  flowing with such a rapidity  $y$  will have a momentum  $(p^0, p^1) = (mu^0, mu^1) = (m \cosh y, m \sinh y)$ .

It is convenient to introduce the light-cone coordinates  $t_+$  and  $t_-$

$$t_+ = t + z, \quad (3.6a)$$

$$t_- = t - z, \quad (3.6b)$$

and their logarithmic representations  $(y_+, y_-)$  defined by

$$y_{\pm} = \ln\{t_{\pm}/\Delta\} = \ln\{(t \pm z)/\Delta\}. \quad (3.7)$$

The advantage of using these variables is that the hydrodynamical equations and the corresponding solutions are quite simple in these variables. The knowledge of the fluid energy density  $\epsilon$  and the flow rapidity  $y$ , as a function of  $(t_+, t_-)$  or  $(y_+, y_-)$  will provide a complete hydrodynamical description of the whole system.

Exercise (1.1) shows that the hydrodynamical equations (3.1) and (3.2) become

$$\frac{\partial \epsilon}{\partial t_+} + 2 \frac{\partial(\epsilon e^{-2y})}{\partial t_-} = 0, \quad (3.8a)$$

$$2 \frac{\partial(\epsilon e^{2y})}{\partial t_+} + \frac{\partial \epsilon}{\partial t_-} = 0. \quad (3.8b)$$

The  $t_+$  and  $t_-$  coordinates are light-like because they lie on the light cone. If we view the  $t_+$  coordinate as approaching time-like and the  $t_-$  as approaching space-like, then the first equation can be considered the equation of continuity and the second the Euler equation of the hydrodynamical current. Conversely, if we view the  $t_-$  coordinate as approaching time-like and the  $t_+$  as approaching space-like, then the second equation can be considered the equation of continuity and the first the Euler equation of the hydrodynamical current.

For the first stage of one-dimensional hydrodynamics, the exact solution for an initially uniform slab has been obtained [3] and discussed in [2, 3, 4, 5, 6, 7, 8, 9, 10, 11, 12]. There is in addition an approximate particular solution that is very simple and applicable to the bulk part of the fluid [1, 2]. In view of the matching of the solution to an approximate three-dimensional motion in the second stage, it suffices to consider the approximate solution of longitudinal hydrodynamical expansion in the present discussions.

The approximate particular solution of the hydrodynamical equation is [2]

$$\epsilon(y_+, y_-) = \epsilon_0 \exp \left\{ -\frac{4}{3}(y_+ + y_- - \sqrt{y_+ y_-}) \right\}, \quad (3.9a)$$

$$y(y_+, y_-) = (y_+ - y_-)/2. \quad (3.9b)$$

The rapidity solution can also be written alternatively as

$$e^{2y(y_+, y_-)} = \frac{t_+}{t_-} = \frac{t+z}{t-z}. \quad (3.10)$$

The corresponding velocity field  $u^0$  is related to the fluid coordinates by

$$u^0(y_+, y_-) = \frac{t}{\sqrt{t-z}\sqrt{t+z}}. \quad (3.11)$$

The constant  $\epsilon_0$  in Eq. (3.9a) is related to the initial energy density at  $(y_{+0}, y_{-0})$  by

$$\epsilon_0 = \epsilon(y_{+0}, y_{-0}) e^{\phi_0}, \quad (3.12)$$

where  $\phi_0$  is

$$\phi_0 = \frac{4}{3}(y_{+0} + y_{-0} - \sqrt{y_{+0} y_{-0}}). \quad (3.13)$$

We can easily prove by direct substitution that (3.9a) and (3.9b) (or (3.10)) are approximate particular solutions of the hydrodynamical equations (3.8a) and (3.8b). First, substituting Eq. (3.10) into the hydrodynamical equations, we obtain

$$\frac{\partial \epsilon}{\partial t_+} + 2 \left[ \frac{\partial \epsilon}{\partial t_-} + \frac{1}{t_-} \right] \frac{t_-}{t_+} = 0, \quad (3.14a)$$

$$2 \left[ \frac{\partial \epsilon}{\partial t_+} + \frac{1}{t_+} \right] \frac{t_+}{t_-} + \frac{\partial \epsilon}{\partial t_-} = 0. \quad (3.14b)$$

We write out  $t_-/t_+$  in the second equation and substitute it into the first equation, and we get

$$\frac{\partial \epsilon}{\partial t_+} \frac{\partial \epsilon}{\partial t_-} - 4 \left[ \frac{\partial \epsilon}{\partial t_-} + \frac{1}{t_-} \right] \left[ \frac{\partial \epsilon}{\partial t_+} + \frac{1}{t_+} \right] = 0 \quad (3.15)$$

We multiply this expression by  $t_+t_-$  and change into the logarithm variables  $y_+$  and  $y_-$ , then the above equation becomes

$$\frac{\partial \epsilon}{\partial y_+} \frac{\partial \epsilon}{\partial y_-} - 4 \left[ \frac{\partial \epsilon}{\partial y_-} + 1 \right] \left[ \frac{\partial \epsilon}{\partial y_+} + 1 \right] = 0 \quad (3.16)$$

If we now substitute Eq. (3.9a) for  $\epsilon$  into the lefthand side of the above equation, we find that the lefthand side gives zero, indicating that Eqs. (3.9a) and (3.9b) are indeed the approximate particular solution of the hydrodynamical equation.

The above solutions (3.9a) and (3.9b) are applicable for both positive and negative  $z$  values and contains the proper reflectional symmetry with respect to the interchange of  $y_+$  and  $y_-$ . The solutions are appropriate for the description of the dynamics of the dense hot matter in the first stage of longitudinal expansion. For simplicity, we shall concentrate our attention on one of the two symmetric sides, the side with positive  $z$ .

The simple approximate solution of (3.9a) and (3.9b) have limitations. Because of the nature of the approximate solution, it cannot describe the boundary layer for which  $t - z < \Delta$  and  $y_-$  becomes negative. At the boundary layer, thermodynamical quantities such as the energy density and the entropy density decrease rapidly and it is not included into the region for the applications of the solution of Eqs. (3.9a). In highly relativistic collisions  $\Delta/a$  is given by  $(2m_p/\sqrt{s_{NN}})$ , which is a small quantity. The region excluded from the approximate solution is not significant in a general description of the fluid.

There is another minor disadvantage of the solution. Because of the nature of the solution for the bulk matter, the solution in Eq. (3.9a) provides only limited choice on the initial conditions, within the form as specified by the simple functions in these equations. However, the dynamics of the system is likely to be insensitive to the fine characteristics of the initial density distribution of the contracted disk of thickness  $\Delta$  along the longitudinal direction. A thin slab of matter of the right dimensions within the Landau model will likely capture the dominant features of the evolution dynamics.

The solutions  $\epsilon(t_+, t_-)$  and  $y(t_+, t_-)$  can be transformed into  $\epsilon(t, z)$  and  $y(t, z)$  by a simple change of variables. We show the solution  $\epsilon(t, z)$  and  $y(t, z)$  as a function of  $z/\Delta$  for different  $t$  in Fig. 2(a) and 2(b) respectively. As one observes, the maximum energy density decreases nearly inversely as a function of  $t$ . One notes that the energy density in the central region decreases in time approximately as  $1/t$ , as the matter expands outward. The flow rapidity is initially close to zero. As the bulk matter expands longitudinally, the magnitude of the rapidity field increases at large values of  $|z|/\Delta$ . We show the velocity field  $u^0(t, z)$  and the corresponding longitudinal velocity  $v_z(t, z)$  as a function of

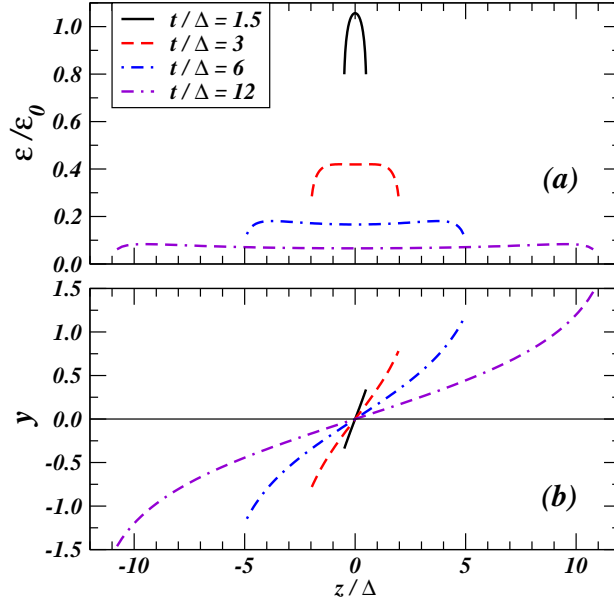


FIG. 3: Approximate Landau hydrodynamical solution of the one-dimensional longitudinal expansion of the system with initial energy density  $\epsilon_0$ , as a function of the longitudinal coordinate  $z$  and various times  $t$  in unit of the slab thickness  $\Delta$ .

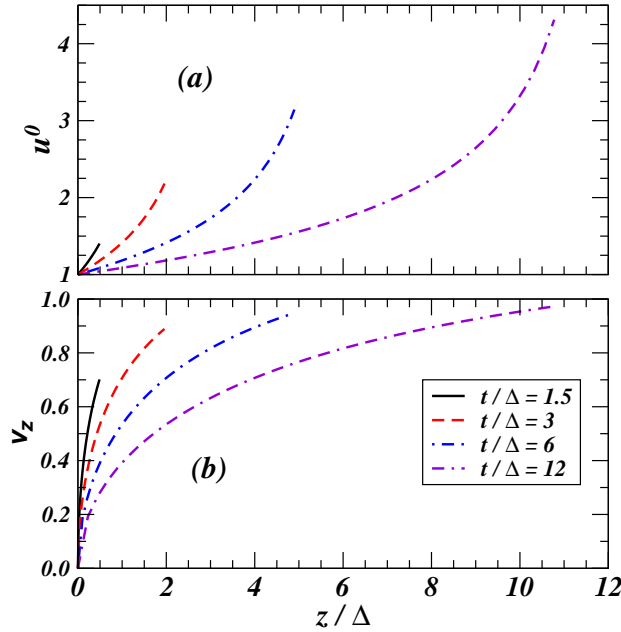


FIG. 4: The proper velocity  $u^0$  and the velocity  $v_z$  along the longitudinal  $z$ -direction as a function of  $z$  and  $t$  Landau hydrodynamics.

$z/\Delta$  for different  $t$  in Fig. 3(a) and 3(b). The magnitude of the longitudinal velocity of the fluid is large at the region of  $|z|$  close to  $t$ .

The hydrodynamical solution Eq. (3.9a) can be equivalently expressed as a function of any other two independent variables. In our problem, it is desirable to use the variables  $t$  and  $y$  because the condition for the transverse displacement to exceed the initial transverse dimension is most conveniently written for a fixed time  $t$ , and the dynamics after the transversality condition is satisfied leads to the freezing of the rapidity  $y$ .

In terms of the  $(t, y)$  variables, we can express  $y_{\pm}$  as

$$y_{\pm} = \ln(t/\cosh y \Delta) \pm y. \quad (3.17)$$

Therefore the hydrodynamical solution Eq. (3.9a) can be re-written in terms of  $(t, y)$  as

$$\epsilon(t, y) = \epsilon_0 \exp \left\{ -\frac{4}{3} (2 \ln(t/\cosh y \Delta) - \sqrt{[\ln(t/\cosh y \Delta)]^2 - y^2}) \right\}, \quad (3.18a)$$

$$z(t, y) = t \sinh y / \cosh y. \quad (3.18b)$$

We can further express the solution as a function of  $(\tau, y)$  to compare Landau hydrodynamics with Bjorken hydrodynamics. We make the transformation

$$t = \tau \cosh y, \quad (3.19a)$$

$$z = \tau \sinh y. \quad (3.19b)$$

We then have

$$y_{\pm} = \ln(\tau/\Delta) \pm y. \quad (3.20)$$

The energy density in Landau hydrodynamics, expressed in terms of  $\tau$  and  $y$  is then

$$\epsilon(\tau, y) = \epsilon_0 \exp \left\{ -\frac{4}{3} \left[ 2 \ln(\tau/\Delta) - \sqrt{[\ln(\tau/\Delta)]^2 - y^2} \right] \right\}. \quad (3.21)$$

In the region  $y \ll \ln(\tau/\Delta)$ , we have

$$\epsilon(\tau, y) = \epsilon_0 \exp \left\{ -\frac{4}{3} \ln(\tau/\Delta) \right\} \propto \frac{1}{\tau^{4/3}}, \quad (3.22)$$

which is the Bjorken hydrodynamics results. Therefore, in the region of small rapidities with  $|y| \ll \ln(\tau/\Delta)$ , Landau hydrodynamics and Bjorken hydrodynamics coincide. However, in other regions when  $|y|$  is not very smaller in comparison with  $\ln(\tau/\Delta)$ , the two types of hydrodynamics differ. In general, because Landau hydrodynamics covers a wider range of rapidities which may not be small, it is a more realistic description for the evolution of the hydrodynamical system.

⊕[ Exercise 1.1 Show that the hydrodynamical equations for  $\epsilon$  and  $y$  are given by Eqs. (3.8a) and (3.8b).

The energy momentum tensor  $T^{00}$  is equal to

$$\begin{aligned} T^{00} &= (\epsilon + p)u^0 u^0 - p \\ &= (\epsilon + p) \cosh^2 y - p. \end{aligned} \quad (3.23)$$

Upon using the equation of state  $p = \epsilon/3$  in Eq. (3.4), the energy momentum tensor can be expressed in terms of  $\epsilon$  and  $y$ .

$$T^{00} = \epsilon(\cosh^2 y + \frac{1}{3} \sinh^2 y). \quad (3.24)$$

We have also,

$$\begin{aligned} T^{01} &= (\epsilon + p)u^0 u^1 \\ &= (4/3)\epsilon \cosh y \sinh y, \end{aligned} \quad (3.25)$$

$$\begin{aligned} T^{11} &= (\epsilon + p)u^1 u^1 + p \\ &= \epsilon(\sinh^2 y + \frac{1}{3} \cosh^2 y). \end{aligned} \quad (3.26)$$

The transformation of  $(t, z)$  to  $(t_+, t_-)$  lead to the following relation between the derivatives,

$$\frac{\partial}{\partial t} = \frac{\partial t_+}{\partial t} \frac{\partial}{\partial t_+} + \frac{\partial t_-}{\partial t} \frac{\partial}{\partial t_-} = \frac{\partial}{\partial t_+} + \frac{\partial}{\partial t_-}. \quad (3.27)$$

$$\frac{\partial}{\partial z} = \frac{\partial t_+}{\partial z} \frac{\partial}{\partial t_+} + \frac{\partial t_-}{\partial z} \frac{\partial}{\partial t_-} = \frac{\partial}{\partial t_+} - \frac{\partial}{\partial t_-}. \quad (3.28)$$

Therefore, Eqs. (3.1) and (3.2) become

$$\frac{dT^{00}}{dt} + \frac{dT^{01}}{dz} = \frac{\partial}{\partial t_+} \left[ \frac{4}{3} \epsilon \sinh y \cosh y + \epsilon (\cosh^2 y + \frac{1}{3} \sinh^2 y) \right] + \frac{\partial}{\partial t_-} \left[ -\frac{4}{3} \epsilon \sinh y \cosh y + \epsilon (\cosh^2 y + \frac{1}{3} \sinh^2 y) \right]. \quad (3.29)$$

$$\frac{dT^{01}}{dt} + \frac{dT^{11}}{dz} = \frac{\partial}{\partial t_+} \left[ \frac{4}{3} \epsilon \sinh y \cosh y + \epsilon (\sinh^2 y + \frac{1}{3} \cosh^2 y) \right] + \frac{\partial}{\partial t_-} \left[ \frac{4}{3} \epsilon \sinh y \cosh y - \epsilon (\sinh^2 y + \frac{1}{3} \cosh^2 y) \right]. \quad (3.30)$$

By forming the difference of the above two equations, we get

$$\frac{\partial}{\partial t_+} [\epsilon (\cosh^2 y + \frac{1}{3} \sinh^2 y)] + \frac{\partial}{\partial t_-} [-\frac{8}{3} \epsilon \sinh y \cosh y + \frac{4}{3} \epsilon (\cosh^2 y + \sinh^2 y)] = 0. \quad (3.31)$$

This can be simplified to be

$$\frac{\partial \epsilon}{\partial t_+} + 2 \frac{\partial (\epsilon e^{-2y})}{\partial t_-} = 0, \quad (3.32)$$

which is Eq. (3.8a). Similarly, by forming the sum of the two equations, we get

$$\frac{\partial}{\partial t_+} \left[ \frac{4}{3} \epsilon (\cosh^2 y + \sinh^2 y) + \frac{8}{3} \epsilon \sinh y \cosh y \right] + \frac{\partial}{\partial t_-} \left[ \frac{2}{3} \epsilon (\cosh^2 y - \sinh^2 y) \right] = 0. \quad (3.33)$$

This leads to

$$2 \frac{\partial (\epsilon e^{2y})}{\partial t_+} + \frac{\partial \epsilon}{\partial t_-} = 0, \quad (3.34)$$

which is Eq. (3.8b). ] ⊕

#### IV. TRANSVERSE EXPANSION

The initial configuration is much thinner in the longitudinal direction than in the transverse directions. Therefore, in the first stage of evolution during the fast one-dimensional longitudinal expansion, there is a simultaneous but slower transverse expansion. The difference in the expansion speeds allows Landau to treat the longitudinal and transverse dynamics as independent expansions. The rate of transverse expansion can then be obtained to provide an approximate description of the dynamics of the system.

We shall consider first the case of a central collision, for which  $a_y = a_x = a$ . The case of non-central collisions will be discussed in Section IX. The transverse expansion is governed by the Euler equation along one of the transverse directions, which can be taken to be along the  $x$  direction,

$$\frac{\partial T^{02}}{\partial t} + \frac{\partial T^{22}}{\partial x} = 0, \quad (4.1)$$

where

$$T^{02} = (\epsilon + p) u^0 u^2 = \frac{4}{3} \epsilon (u^0)^2 v_x, \quad (4.2)$$

and we have used the relation  $u^2 = u^0 v_x$ . The energy-momentum tensor  $T^{22}$  is

$$T^{22} = (\epsilon + p)(u^2)^2 - pg^{22} = \frac{4}{3}\epsilon(u^0)^2(v_x)^2 + p. \quad (4.3)$$

As the transverse expansion is relatively slow, we can neglect the first term on the righthand side of the above expression and keep only the pressure term  $p$ .

In Landau's method of splitting the equations, one makes the approximation that during the first stage the quantities  $\epsilon$  and  $y$  as a function of  $t$  and  $z$  have been independently determined in the one-dimensional longitudinal motion. It suffices to use Eq. (4.1) to determine the transverse displacement as a function of time. Equation (4.1) can therefore be approximated as

$$\frac{4}{3}\epsilon(u^0)^2 \frac{\partial v_x}{\partial t} = -\frac{\partial p}{\partial x}. \quad (4.4)$$

The transverse displacement  $x(t)$  (relative to zero displacement) as a function of time  $t$  is related to the acceleration  $\partial v_x/\partial t$  by

$$x(t) = \frac{1}{2} \left( \frac{\partial v_x}{\partial t} \right) t^2. \quad (4.5)$$

The pressure is  $p = \epsilon/3$  at the center of the transverse region and is zero at the radial surface  $a/2$ . Therefore the equation for the displacement is given from Eq. (4.4) by

$$\frac{4}{3}\epsilon(u^0)^2 \frac{2x(t)}{t^2} = \frac{\epsilon}{3a/2}. \quad (4.6)$$

We note that there is a factor of 4 arising from the ratio of  $4\epsilon/3$  from  $(\epsilon + p)$  on the lefthand side relative to  $\epsilon/3$  from the pressure  $p$  on the righthand side. However, in the original formulation of Landau [1, 2], this factor of 4 is taken to be unity for an order of magnitude estimate of the transverse displacement. For our purpose of making quantitative comparison with experimental data, this factor of 4 cannot be neglected. We shall find in Section 5 and 6 that the presence of this factor of 4 leads to the modified rapidity distribution (6.12) that agrees better with experimental  $dN/dy$  data than the Landau distribution of Eq. (1.5).

From Eq. (4.6), the transverse displacement  $x(t)$  during the one-dimensional longitudinal expansion increases quadratically with  $t$  as

$$x(t) = \frac{t^2}{4a(u^0)^2} = \frac{t^2}{4a \cosh^2 y}. \quad (4.7)$$

For a fixed  $t$ , the transverse displacement  $x(t)$  as a function of the rapidity is greatest at  $y = 0$  and it decreases as  $|y|$  increases. The variation of the transverse displacement as a function of rapidity leads to different times when the fluid element enters from the first stage to the second stage of frozen rapidities.

## V. SECOND STAGE OF CONIC FLIGHT

The description of one-dimensional solution of longitudinal expansion with the accompanying transverse expansion in the first stage is applicable as long as the transverse displacement  $x(t)$  is sufficiently small compared with the transverse dimension  $a$ . It ceases to be applicable at the time  $t_m$  when the transverse displacement  $x(t_m)$  is equal to the transverse dimension  $a$ . Landau suggested

that when  $x(t_m)$  is equal to  $a$  we need to switch to a new type of solution in the second stage of fluid dynamics.

What type of fluid motion is expected after the fluid element enters the second stage? For a fluid element at  $t \geq t_m$ , the transverse displacement  $x(t)$  already has exceeded the initial transverse dimension. With the fluid element beyond the initial transverse dimension, the derivatives of hydrodynamical quantities with respect to both the transverse coordinates and  $t_-$  are small. Because of the smallness of these derivatives, Landau argued that the hydrodynamical forces become so small that they can be neglected in the hydrodynamical equations at these locations. The flow rapidity  $y$  will be frozen for  $t \geq t_m$ . Freezing the rapidity of a fluid element as a function of time is equivalent to freezing the opening polar angle  $\theta$  between the fluid trajectory and the collision axis at these longitudinal locations. The motion of the fluid element with a fixed polar angle can be described as a ‘three-dimensional’ conic flight, with no change of the flow rapidity.

In mathematical terms, Landau’s condition for rapidity freezeout occurs at the time  $t_m(y)$  when the transverse displacement satisfies [1, 2]

$$x(t_m) = a, \quad (5.1)$$

which, as determined from Eqs. (4.7) and (5.1), takes place at

$$t_m(y) = 2au^0 = 2a \cosh y. \quad (5.2)$$

The switching time  $t_m(y)$  increases with increasing magnitude of the rapidity.

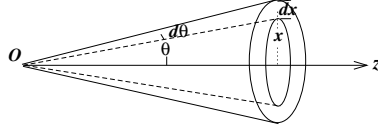


FIG. 5: Schematic picture of the opening polar angle  $\theta$  between the fluid element trajectory and the longitudinal axis. The conic energy and entropy within the angle element  $d\theta$  is preserved in this second stage of conic flight,

The solution of the hydrodynamical variables during this second stage of conic flight can be easily obtained. In a conic flight with a cone of opening polar angle  $\theta$  within an angle element  $d\theta$  as shown in Fig. 5, the energy-momentum tensor and the entropy flux within the cone element must be conserved as a function of time. The cross sectional area of such a cone element is  $2\pi x dx$ . So the conservation of energy and entropy conic flow correspond to

$$dE = \epsilon u^0 u^0 2\pi x dx = \text{constant}, \quad (5.3)$$

and

$$dS = \sigma u^0 2\pi x dx = \epsilon^{3/4} u^0 2\pi x dx = \text{constant}, \quad (5.4)$$

where  $\sigma$  is the entropy density. Dividing the first equation by the second equation, we get

$$\epsilon^{1/4} u^0 = \text{constant}, \quad (5.5)$$

which gives

$$\epsilon \propto \frac{1}{(u^0)^4}. \quad (5.6)$$

On the other hand, in the conic flight,  $x$  and  $dx$  are proportional to  $t$ . Hence, Eq. (5.3) gives

$$\epsilon u^0 u^0 t^2 = \text{constant}. \quad (5.7)$$

Eqs. (5.6) and (5.7) yield the dependence of various quantities as a function of  $t$ ,

$$\epsilon \propto \frac{1}{t^4}, \quad \sigma \propto \frac{1}{t^3}, \quad \text{and} \quad u^0 \propto t. \quad (5.8)$$

These equations give the solution of the evolution of the fluid elements as a function of time in the second stage. By matching the solutions at  $t = t_m(y)$ , the energy density and velocity fields at the second stage for  $t > t_m(y)$  is

$$\epsilon(t, y) = \epsilon(t_m, y) t_m^4 / t^4 \quad (5.9a)$$

$$u^0(t, y) = u^0(t_m, y) t / t_m. \quad (5.9b)$$

The velocity component  $u^0$  of a fluid element increases linearly with time in this second stage. In contrast, in the first stage, the velocity component  $u^0$  of a fluid element with fixed  $t - z$  and  $z$  comparable to  $t$  increase with time only approximately as  $t^{1/2}$ , as indicated by Eq. (3.11). Thus, the fluid element approaches the speed of light faster in the second stage than in the first stage.

## VI. RAPIDITY DISTRIBUTION IN HIGH ENERGY HEAVY-ION COLLISIONS

The picture that emerges from Landau hydrodynamics can be summarized as follows. For an initial configuration of a thin disk of dense matter at a high temperature and pressure, the first stage of the motion is a one-dimensional longitudinal expansion with a simultaneous transverse expansion. The transverse expansion lead to a transverse displacement. When the magnitude of the transverse displacement exceeds the initial transverse dimension, forces acting on the fluid element becomes small and the fluid elements will proceed to the second stage of conic flight with a frozen rapidity. As the transverse displacement depends on rapidity, and the transverse displacement magnitude increases with increasing rapidity magnitude, the moment when the fluid element switches from the first stage to the second stage depends on the rapidity. The final rapidity distribution of particles is therefore given by the rapidity distribution of the particles at the matching time  $t_m(y)$ .

We shall first evaluate the entropy distribution as a function of rapidity  $y$  and time  $t$  in the first stage of hydrodynamics. Consider a slab element  $dz$  at  $z$  at a fixed time  $t$ . The entropy within the slab element is

$$dS = \sigma u^0 dz. \quad (6.1)$$

Using the solution (3.10), we can express  $z$  as a function of  $t$  and rapidity  $y$  during the one-dimensional longitudinal expansion,

$$z = t \sinh y / \cosh y. \quad (6.2)$$

For a fixed value of  $t$ , we therefore obtain

$$\begin{aligned} dS &= \sigma u^0 t dy / \cosh^2 y \\ &= \sigma t dy / \cosh y. \end{aligned} \quad (6.3)$$

The entropy density  $\sigma$  is related to  $\epsilon$  by  $\sigma = c\epsilon^{3/4}$  and  $\epsilon$  is given by (3.9a). We obtain the entropy element at the time  $t$ ,

$$dS = c\epsilon_0^{3/4} \exp\{-(y_+ + y_- - \sqrt{y_+ y_-})\} t dy / \cosh y. \quad (6.4)$$

In the second stage, different fluid elements with different rapidities switch to conic flight at different time  $t_m(y)$ . The rapidity is frozen after  $t > t_m(y)$ . The entropy element after freezeout needs to be evaluated at the switching time  $t = t_m(y)$

$$dS = c\epsilon_0^{3/4} \left[ \exp\{-(y_+ + y_- - \sqrt{y_+ y_-})\} \frac{t}{\cosh y} \right]_{t=t_m(y)} dy \quad (6.5)$$

To evaluate the square-bracketed quantity at  $t = t_m(y)$ , we obtain from Eq. (3.7) and (6.2) that

$$e^{y_{\pm}} = \frac{t}{\Delta} \frac{e^{\pm y}}{\cosh y}. \quad (6.6)$$

Therefore, we have

$$e^{y_{\pm}} \Big|_{t=t_m(y)} = \frac{t_m(y)}{\Delta} \frac{e^{\pm y}}{\cosh y} = \frac{2a}{\Delta} e^{\pm y}, \quad (6.7)$$

which gives

$$y_{\pm} \Big|_{t=t_m(y)} = \ln(2a/\Delta) \pm y. \quad (6.8)$$

We note that

$$\ln(2a/\Delta) = y_b = L + \ln 2, \quad (6.9)$$

where  $y_b$  is the beam rapidity in the center-of-mass system,

$$y_b = \cosh^{-1}(\sqrt{s_{NN}}/2m_p) \doteq \ln(\sqrt{s_{NN}}/m_p). \quad (6.10)$$

The entropy element of Eq. (6.5) is therefore

$$dS = c\epsilon_0^{3/4} 2a \exp\{-2y_b + \sqrt{y_b^2 - y^2}\} dy \quad (6.11)$$

As the entropy is proportional to the number of particles, we obtain the rapidity distribution of the particle number

$$\frac{dN}{dy} \propto \exp\{\sqrt{y_b^2 - y^2}\}. \quad (6.12)$$

which differs from Landau's rapidity distribution of Eq. (1.5), with the beam rapidity  $y_b = L + \ln 2$  replacing Landau's  $L$ . Therefore, we find that the rapidity distribution in the center-of-mass system should be modified from the original Landau distribution.

While many steps of the formulation are the same, the main difference between our formulation and Landau's appears to be the additional factor of 2 in Eq. (6.7) and (5.2) in the new formulation. This factor can be traced back to the factor of 4 in the ratio of  $4\epsilon/3$  from  $(\epsilon + p)$  on the left hand side of Eq. (4.6) and  $\epsilon/3$  from the pressure  $p$  on the right hand side. In Landau's formulation, this factor of 4 is taken to be unity for an order-of-magnitude estimate of the transverse expansion. Hence, there can be a modification of Landau's expression for the rapidity distribution.

## VII. COMPARISON OF LANDAU HYDRODYNAMICS WITH EXPERIMENTAL RAPIDITY DISTRIBUTIONS

We would like to compare the modified distribution with the Landau distribution and experimental distributions for central AuAu collisions at various energies [13, 14, 15]. We can evaluate a few quantities to get an idea of the differences. Consider collisions at  $\sqrt{s_{NN}} = 200$  GeV. The beam rapidity  $y_b$  is  $y_b = 5.36$ , and the logarithm of the Lorentz contraction factor is  $L = 4.67$ . The difference between  $y_b$  and  $L$  is substantial and leads to different shapes of the rapidity distributions as one observes in Fig. 6.

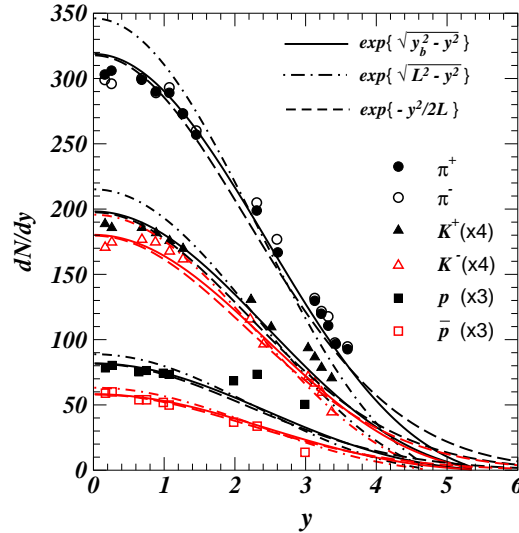


FIG. 6: Comparison of experimental rapidity distribution with theoretical distribution in the form of  $dN/dy \propto \exp\{\sqrt{y_b^2 - y^2}\}$  (solid curves), Landau's distribution  $dN/dy \propto \exp\{\sqrt{L^2 - y^2}\}$  (dashed-dot curves), and the Gaussian  $dN/dy \propto \exp\{-y^2/2L\}$  (dashed curves) for produced particles with different masses. Data are from [13] for AuAu collisions at  $\sqrt{s_{NN}} = 200$  GeV.

Fig. 6 gives the theoretical and experimental rapidity distributions for  $\pi^+$ ,  $\pi^-$ ,  $K^+$ ,  $K^-$ ,  $p$ , and  $\bar{p}$  [13]. The solid curves in Fig. 6 are the results for  $\sqrt{s_{NN}} = 200$  GeV from the modified distribution Eq. (6.12) with the  $y_b$  parameter, whereas the dashed curves are the Landau distribution of Eq. (1.5),  $dN/dy \propto \exp\{\sqrt{L^2 - y^2}\}$  with the  $L$  parameter. The theoretical distributions for different types of particles have been obtained by keeping the functional forms of the distribution and fitting a normalization constant to match the experimental data. We observe that Landau rapidity distributions are significantly narrower than the experimental rapidity distributions, whereas the modified distribution Eq. (6.12) gives theoretical results that agree better with experimental data.

As a further comparison, we show theoretical distributions calculated with the Gaussian distribution of Eq. (1.3) as the dashed curves. We find that except for the region of large rapidities, the Gaussian distributions is a good representation of the modified Landau distribution. The close similarity between the modified distribution (6.12) and the Gaussian distribution (1.3) explains the puzzle mentioned in the Introduction. The Gaussian distribution and the original Landau distribution are different distributions. Past successes of the Gaussian distribution in explaining experimental rapidity data [13, 14, 15] arises, not because it is an approximation of the original Landau distribution (1.5), but because it is in fact close to the modified Landau distribution (6.12) that derives its support from a careful re-examination of Landau hydrodynamics.

We compare theoretical distributions with the  $\pi^-$  rapidity distribution for collisions at various energies. The solid curves in Fig. 7 are the results from the modified distribution Eq. (6.12) with

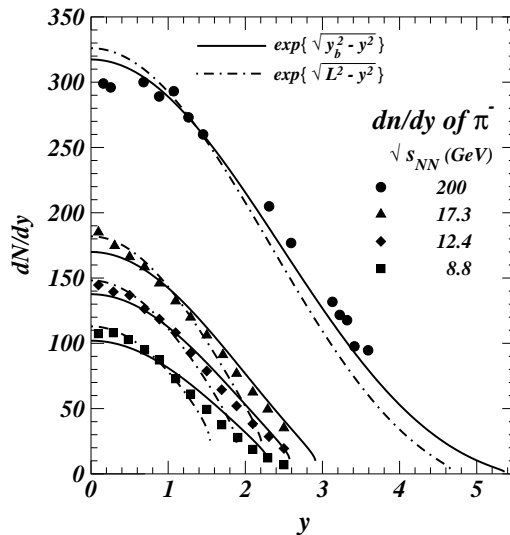


FIG. 7: Comparison of experimental rapidity distribution with theoretical distribution in the form of  $dN/dy \propto \exp\{\sqrt{y_b^2 - y^2}\}$  (solid curves) and Landau's distribution  $dN/dy \propto \exp\{\sqrt{L^2 - y^2}\}$  (dashed curves) for produced particles at different energies. Data are from the compilations in [13].

the  $y_b$  parameter, whereas the dashed curves are the Landau distribution of Eq. (1.5) with the  $L$  parameter. The experimental data are from the compilation of [13]. The modified distribution of Eq. (6.12) appears to give a better agreement with experimental data than the Landau distribution when all the data points at all energies are considered.

While the comparison of the modified distribution gives a better agreement with experimental data than the original Landau distribution, it should be pointed out that the agreement can be further improved. Landau's condition of rapidity freezeout, Eq. (5.1), is only a close estimate that already goes a long way in providing a good description. It may however admit refinement beyond the first estimate. We can in fact use the experimental data to guide us for a better estimate of the rapidity freezeout condition which can be conveniently modified to be

$$x(t_m) = \zeta a, \quad (7.1)$$

where  $\zeta$  is of order unity but can allow small deviations from unity. In this case, the matching time becomes

$$t_m(y) = 2\sqrt{\zeta}a \cosh y, \quad (7.2)$$

and the rapidity distribution becomes

$$dN/dy \propto \exp\{\sqrt{[y_b + (\ln \zeta)/2]^2 - y^2}\}. \quad (7.3)$$

The comparison in Figs. 6 and 7 for the  $\pi^\pm$  distributions indicates that a parameter  $\zeta$  slightly greater than unity will lead to a better agreement with experiment.

## VIII. PREDICTIONS OF PARTICLE RAPIDITY DISTRIBUTION FOR LHC ENERGIES

We can re-write the rapidity distribution of charged particles in terms of the normalized distribution  $dF/dy$

$$(dN_{ch}/dy)/(N_{\text{part}}/2) = [N_{ch}/(N_{\text{part}}/2)]dF/dy. \quad (8.1)$$

The normalized distribution  $dF/dy$  is

$$\frac{dF}{dy} = \begin{cases} A_{\text{norm}} \exp\{\sqrt{y_b^2 - y^2}\} & \text{for modified Landau distribution,} \\ A_{\text{norm}} \exp\{\sqrt{L^2 - y^2}\} & \text{for Landau distribution,} \\ A_{\text{norm}} \exp\{-y^2/2L\} & \text{for Gaussian Landau distribution,} \end{cases} \quad (8.2)$$

where  $A_{\text{norm}}$  is a normalization constant such that

$$\int dF/dy = 1. \quad (8.3)$$

As we remarked earlier, the approximate Landau hydrodynamical model is restricted in the region of  $|y| < y_b$  for the modified distribution and  $L < |y|$  for the original Landau distribution. The neglect of the tail region of the distribution will not affect significantly the distribution and its normalization.

With the knowledge of the total charged multiplicity from Fig. 1, and the shape of the rapidity distribution from Eq. (8.2), we can calculate  $dN_{\text{ch}}/dy/(N_{\text{part}}/2)$  as a function of rapidity. Fig. 5 gives the predicted rapidity distributions at LHC energies. For heavy-ion collisions at  $\sqrt{s_{NN}} = 5.5$  TeV with full stopping ( $\xi = 1$ ), the maximum value of  $dN/dy$  per participant pair is about 22 at midrapidity. For  $pp$  collisions at  $\sqrt{s_{NN}} = 14$  TeV with  $\xi = 0.5$ , the maximum  $dN/dy$  is approximately 24 at  $y = 0$ . The widths of the rapidity distributions are  $\sigma_y \sim 3$ . The solid curves are for the modified distribution, the dashed-dot curves are for the original Landau distribution, and the dashed curves are for the Gaussian distribution. These results provide useful theoretical data for comparison with future experiments.

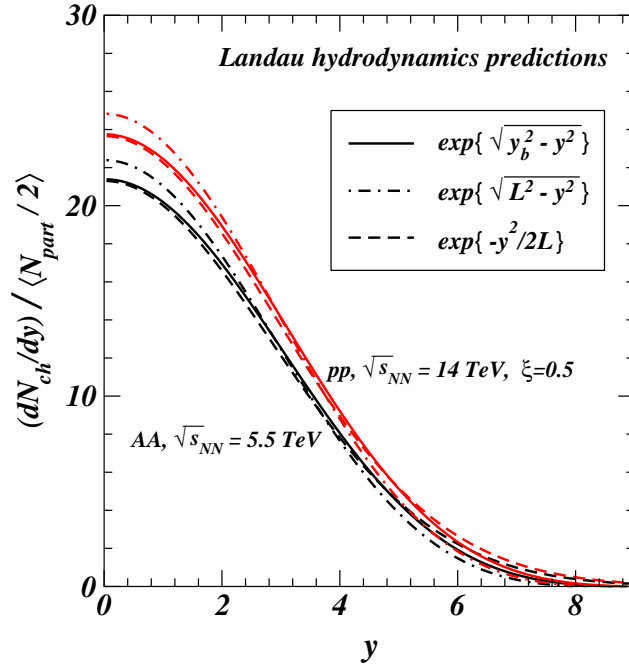


FIG. 8: The predicted rapidity distributions  $dN_{\text{ch}}/dy/(N_{\text{part}}/2)$  of charged particles produced in (i)  $pp$  collisions at  $\sqrt{s_{NN}} = 14$  TeV with  $\xi = 0.5$ , and (ii) AA collisions at  $\sqrt{s_{NN}} = 5.5$  TeV with full stopping ( $\xi = 1$ ), in Landau hydrodynamics. The solid curves are obtained with the modified distribution, the dashed-dot curves are obtained with the original Landau distribution, and the dashed curves with the Gaussian distribution.

## IX. GENERALIZATION TO NON-CENTRAL COLLISIONS

We have considered so far the case of central collision, for which the dimensions in all directions before Lorentz contraction are all equal. In non-central collisions, the transverse radius  $a_\phi/2$  will depend on the azimuthal angle  $\phi$  measured relative to the  $x$  axis as depicted in Fig. 1.

We can easily generalize the Landau model to the case of non-central collisions. The first stage of longitudinal expansion proceeds in the same way. The initial energy density  $\epsilon_0$  will need to be adjusted as it depends on the impact parameter. The important quantity is however the temporal dependence of the transverse displacement. Following the same Landau arguments as in the central collision case, Eq. (4.6) for the transverse displacement can be generalized to the non-central collision case to be

$$\frac{4}{3}\epsilon(u^0)^2\frac{2\rho(\phi, t)}{t^2} = \frac{\epsilon}{3a_\phi/2}. \quad (9.1)$$

where  $\rho(\phi, t)$  is the transverse displacement at azimuthal angle  $\phi$ . As a consequence, the transverse displacement depend on  $\phi$  and  $t$  as

$$\rho(\phi, t) = \frac{t^2}{4a_\phi(u^0)^2} = \frac{t^2}{4a_\phi \cosh^2 y}. \quad (9.2)$$

We can set up the Landau condition for the onset of the second stage as the condition that the transverse displacement  $\rho(\phi, t)$  is equal to the transverse dimension  $a_\phi$ ,

$$\rho(\phi, t_m) = a_\phi. \quad (9.3)$$

Thus, in the case of non-central collision, the Landau condition of (5.1) is changed to

$$t_m(y, \phi) = (a_\phi/a) \times 2a \cosh y, \quad (9.4)$$

which shows that the rapidity freezeout time  $t_m$  is reduced by the factor  $(a_\phi/a)$ , compared to the freezeout time for central collisions. For a fixed azimuthal angle  $\phi$ , fluid elements go from the first stage motion to the second stage motion at different times. The matching time  $t_m$  (the rapidity freezeout time) occurs at different instances for different rapidities. Following the same argument as before, Eq. (6.8) for the non-central collision case becomes

$$y_\pm|_{t=t_m(y, \phi)} = \ln(a_\phi/a) + \ln(2a/\Delta_b) \pm y, \quad (9.5)$$

where the longitudinal thickness of the initial slab  $\Delta_b$  depends on the impact parameter  $b$ . As a consequence, the rapidity distribution for this non-central collision is

$$\frac{dN}{dy} \propto \exp\{\sqrt{[\ln(2a/\Delta_b) + \ln(a_\phi/a)]^2 - y^2}\}. \quad (9.6)$$

## X. CONCLUSIONS AND DISCUSSIONS

In many problems in high-energy collisions such as in the description of the interaction of the jet or quarkonium with the produced dense matter, it is desirable to have a realistic but simple description of the evolution of the produced medium. Landau hydrodynamics furnishes such a tool for this purpose.

Recent successes of Landau hydrodynamics [13, 14, 15] in explaining the rapidity distribution, total particle multiplicities, and limiting fragmentation indicate that it contains promising degrees of freedom. Questions are however raised concerning the use of pseudorapidity or rapidity variables, the approximate Gaussian form or the square-root exponential form of the rapidity distribution, and the values of the parameters in the rapidity distribution.

We start with the rapidity variable from the outset so that we do not need to worry about the question of the rapidity or the pseudorapidity variable. We follow the formulation of the Landau hydrodynamics by keeping careful track of the numerical constants that enter into the derivation. We confirm Landau's central results except that the approximate rapidity distribution obtained by Landau needs to be modified, when all numerical factors are carefully tracked. In particular, the rapidity distribution in the center-of-mass system should be more appropriately given as  $dN/dy \propto \exp\{\sqrt{y_b^2 - y^2}\}$ , where  $y_b$  is the beam nucleon rapidity, instead of the Landau original result of  $dN/dy(\text{Landau}) \propto \exp\{\sqrt{L^2 - y^2}\}$ . The modified distribution leads to a better description of the experimental data, thereby supports the approximate validity of Landau hydrodynamics as a description of the evolution of the produced bulk matter. Phenomenological fine-tuning can be further introduced as in Eqs. (7.2) and (7.3) to relate the rapidity freezeout time  $t_m$  with the rapidity and transverse radius.

The modified distribution differs only slightly from the Gaussian distribution  $dN/dy(\text{Gaussian}) \propto \exp\{-y^2/2L\}$ , that has been used successfully and extensively in the literature [13, 14, 15, 16, 17]. This explains the puzzle we mention in the Introduction. Even though the Gaussian Landau distribution (1.3) is conceived as an approximate representation of the original Landau distribution (1.5) for the region of small rapidity with  $|y| \ll L$ , it differs from the original Landau distribution in other rapidity regions. They are in fact different distributions. The Gaussian distribution has been successfully used to explain experimental rapidity distribution data [13, 14, 15], not because it is an approximation of the original Landau distribution (1.5), but because it is in fact a good representation of the modified Landau distribution (6.12) that derives its support from a careful re-examination of Landau hydrodynamics. Thus, there is now a firmer theoretical support for the Gaussian distribution (1.3) owing to its similarity to the modified distribution of (6.12).

The need to modify Landau's original distribution should not come as a surprise, as the original distribution was intended to be qualitative. Our desire to apply it quantitatively therefore lead to a more stringent re-examination, with the result of the modification as we suggest.

The quantitative successes of the modified Landau hydrodynamics make it a useful tool for many problems in high-energy heavy-ion collisions. We can now view with some degree of confidence Landau's picture for the evolution of the bulk matter. The evolution first proceeds with a one-dimensional longitudinal expansion with a simultaneous transverse expansion. Different parts of the fluid is subject to different transverse displacements. Those in the central rapidity receive the greatest transverse displacement and will freeze out in  $y$  at the earliest. The final distribution is obtained by collecting the bulk matter at different times of rapidity freezeout.

In spite of these successes, many problems will need to be examined to make the Landau model an even better tool. We can here outline a few that will need our attention. The distribution so far deals with flow rapidity of the fluid elements, and the thermal distribution of the particles inside the fluid element has not been included. The folding of the thermal distribution of the particles will broaden the rapidity distribution and should be the subject of future investigations. Another improvement is to work with a curvilinear coordinate system in the transverse direction to obtain the transverse displacement. This will improve the description of the matching time in the transverse direction. One may wish to explore other forms of the freezeout condition instead of Landau's transverse displacement condition, to see how sensitive the results can depend on the freezeout condition. Finally, as the approximate solution for the one-dimensional is also available, it may also

be of interest to see how much improvement there can be in obtaining the matching time estimates which enter into the rapidity freeze-out condition.

The author wishes to thank Prof. D. Blaschke for his hospitality at the the Helmholtz International Summer School, Bogoliubov Laboratory of Theoretical Physics, Dubna, Russia. This research was supported in part by the Division of Nuclear Physics, U.S. Department of Energy, under Contract No. DE-AC05-00OR22725, managed by UT-Battelle, LLC.

- 
- [1] L. D. Landau, *Izv. Akad. Nauk SSSR* **17**, 51 (1953).
  - [2] S. Z. Belenkij and L. D. Landau, *Usp. Fiz. Nauk* **56**, 309 (1955); *Nuovo Cimento, Suppl.* **3**, 15 (1956).
  - [3] I. M. Khalatnikov, *Zh. Eksp. Teor. Fiz.* **27**, 529 (1954).
  - [4] S. Z. Belenkij and G. A. Milekhin, *Zh. Eksp. Teor. Fiz.* **29**, 20 (1956) [*Sov. Phys. JETP* **2**, 14 (1956)]; I. L. Rosental, *Zh. Eksp. Teor. Fiz.* **31**, 278 (1957) [*Sov. Phys. JETP* **4**, 217 (1959)]; G. A. Milekhin, *Zh. Eksp. Teor. Fiz.* **35**, 978 (1958) [*Sov. Phys. JETP* **8**, 682 (1959)]; G. A. Milekhin, *Zh. Eksp. Teor. Fiz.* **35**, 1185 (1958) [*Sov. Phys. JETP* **8**, 829 (1959)].
  - [5] S. Amai, H. Fukuda, C. Iso, and M. Sato, *Prog. Theo. Phys.* **17**, 241 (1957).
  - [6] D. K. Srivastava, J. Alam, B. Sinha, *Phys. Lett.* **B296**, 11 (1992); D. K. Srivastava, Jan-e Alam, S. Chakrabarty, B. Sinha, S. Raha, *Ann. Phys.* **228**, 104 (1993); D. K. Srivastava, J. Alam, S. Chakrabarty, S. Raha, B. Sinha, *Phys. Lett.* **B278**, 225 (1992).
  - [7] Y. Hama, T. Codos, O. Scoliosis's, *Braz. J. Phys.* **35**, 24 (2005) [arXiv:hep-ph/0407264]; C. E. Aguiar, T. Kodama, T. Osada, Y. Hama, *J. Phys. G* **27**, 75 (2001).
  - [8] S. Pratt, *Phys. Rev.* **C75**, 024907 (2007).
  - [9] A. Bialas, R. A. Janik, and R. Peschanski, *Phys. Rev.* **C76**, 054901 (2007), [arXiv:0706.2108].
  - [10] T. Csörgö, M. I. Nagy, and M. Csanád, *Phys. Lett.* **B663**, 306 (2008), [nucl-th/0706.2108].
  - [11] M. I. Nagy, T. Csörgö, and M. Csanád, *Phys. Rev.* **C77**, 3024908 (2008).
  - [12] G. Beuf, R. Peschanski, and E. Saridakis, arXiv:0808.1073.
  - [13] M. Murray for the Brahms Collaboration, *J. Phys. G* **30**, S667 (2004)
  - [14] P. Steinberg, *Nucl. Phys.* **A752**, 423 (2005).
  - [15] P. Steinberg, *Proceedings of 3rd International Workshop on Critical Point and Onset of Deconfinement, Florence, Italy, 3-6 Jul 2006.* arXiv:nucl-ex/0702019.
  - [16] W. Busza, *Acta Phys. Polon.* **B35**, 2873 (2004).
  - [17] P. Carruthers and Minh Doung-van, *Phys. Rev.* **8**, 859 (1973).
  - [18] E. K. G. Sarkisyan, A.S. Sakharov, *AIP Conf.Proc.* **828**, 35 (2006), [hep-ph/0510191]; E. K. G. Sarkisyan, A.S. Sakharov, [hep-ph/0410324].
  - [19] C. Y. Wong, *Introduction to High-Energy Heavy-Ion Collisions*, World Scientific Publisher, 1994.
  - [20] S. Chadha, C. S. Lam, and Y. C. Leung, *Phys. Rev. D* **10**, 2817 (1974).
  - [21] C. Y. Wong and T. A. Welton, *Phys. Lett.* **49B**, 243 (1974).
  - [22] M. Basile *et al.*, *Nuovo Cim.* **65A**, 400 (1981); M. Basile, *Nuovo Cim.* **67A**, 244 (1981).